

## Opening of Size-Selective Pores in Endosomes during Human Rhinovirus Serotype 2 In Vivo Uncoating Monitored by Single-Organelle Flow Analysis

Marianne Brabec,<sup>1</sup> Daniela Schober,<sup>1</sup> Ernst Wagner,<sup>2</sup> Nora Bayer,<sup>1†</sup>  
Robert F. Murphy,<sup>3</sup> Dieter Blaas,<sup>4</sup> and Renate Fuchs<sup>1\*</sup>

*Department of Pathophysiology, Center for Physiology and Pathophysiology,<sup>1</sup> and Max F. Perutz Laboratories, University Departments at the Vienna Biocenter, Department of Medical Biochemistry,<sup>4</sup> Medical University of Vienna, Vienna, Austria; Department of Pharmacy, Pharmaceutical Biology-Biotechnology, Ludwig-Maximilians-Universität, Munich, Germany<sup>2</sup>; and Departments of Biological Sciences and Biomedical Engineering, Carnegie Mellon University, Pittsburgh, Pennsylvania<sup>3</sup>*

Received 28 June 2004/Accepted 27 August 2004

**The effect of virus uncoating on endosome integrity during the early steps in viral infection was investigated. Using fluid-phase uptake of 10- and 70-kDa dextrans labeled with a pH-dependent fluorophore (fluorescein isothiocyanate [FITC]) and a pH-independent fluorophore (cyanine 5 [Cy5]), we determined the pHs of labeled compartments in intact HeLa cells by fluorescence-activated cell sorting analysis. Subsequently, the number and pH of fluorescent endosomes in cell homogenates were determined by single-organelle flow analysis. Cointernalization of adenovirus and 70-kDa FITC- and Cy5-labeled dextran (FITC/Cy5-dextran) led to virus-induced endosomal rupture, resulting in the release of the marker from the low-pH environment into the neutral cytosol. Consequently, in the presence of adenovirus, the number of fluorescent endosomes was reduced by 40% compared to that in the control. When human rhinovirus serotype 2 (HRV2) was cointernalized with 10- and 70-kDa FITC/Cy5-dextrans, the 10-kDa dextran was released, whereas the 70-kDa dextran remained within the endosomes, which also maintained their low pH. These data demonstrate that pores are generated in the membrane during HRV2 uncoating and RNA penetration into the cytosol without gross damage of the endosomes; 10-kDa dextran can access the cytosol through these pores. Whereas rhinovirus-mediated pore formation was prevented by the vacuolar ATPase inhibitor bafilomycin A1, adenovirus-mediated endosomal rupture also occurred in the presence of the inhibitor. This finding is in keeping with the low-pH requirement of HRV2 infection; for adenovirus, no pH dependence for endosomal escape was found with this drug.**

Viruses have developed a number of strategies to enter host cells and to transfer their genomes to the site of replication. For most viruses, the whole viral particle, the viral core, or the nucleic acid must overcome at least one membrane barrier to gain access to the cytosol. Enveloped viruses, such as influenza virus, vesicular stomatitis virus, Semliki Forest virus, and many others, fuse their lipid envelope with the endosomal or plasma membrane, resulting in release of the nucleocapsid or genome into the cytosol (25). For some nonenveloped viruses, such as adenovirus, it has been clearly demonstrated that the genome accesses the cytoplasm through disruption of the endosome (27). For poliovirus and the minor-group human rhinoviruses (HRVs) (see below), genome penetration into the cytoplasm presumably occurs through a pore formed in the plasma or endosomal membrane (4, 16). The poliovirus receptor (CD155) not only serves as a vehicle for virus binding but also catalyzes RNA uncoating. Similarly, intercellular adhesion molecule 1 (ICAM-1; CD45), the receptor of the major-group

HRVs (see below), facilitates uncoating in certain serotypes of these HRVs. The more stable serotypes, in addition, require the low pH of endosomes to release their RNAs (32). Poliovirus uncoating and infection are pH independent (33). Therefore, it is conceivable that uncoating occurs directly at the plasma membrane; however, direct evidence for this notion is still lacking, and it is unclear whether poliovirus needs to be endocytosed for infection to occur (6). For minor-group HRV serotype 2 (HRV2), it was shown previously that infection occurs from endosomes in a low-pH-dependent manner (3, 35, 41). The present study was initiated to investigate by which mechanism this virus relocates its genomic RNA into the cytosol, that is, whether HRV2 follows a route similar to that of adenoviruses or translocates its RNA through a pore in the membrane, as is assumed, but not proven, for the closely related poliovirus.

Rhinoviruses belong to the picornavirus family and are composed of 60 copies each of four capsid proteins, VP1 through VP4, enclosing a single-stranded RNA genome of positive polarity within an icosahedral capsid. There are two groups of HRVs. Major-group HRVs bind ICAM-1, which resembles the poliovirus receptor in that it belongs to the immunoglobulin superfamily and catalyzes uncoating (43). Minor-group HRVs, such as HRV2, bind members of the low-density lipoprotein receptor family (15), which mediate internalization but do not

\* Corresponding author. Mailing address: Center for Physiology and Pathophysiology, Medical University of Vienna, Waehringer Guertel 18-20, A-1090 Vienna, Austria. Phone: (43) 1 40 40-5127. Fax: (43) 1 40 40-5130. E-mail: renafe.fuchs@meduniwien.ac.at.

† Present address: PerkinElmer Life & Analytical Sciences, Vienna, Austria.

catalyze uncoating (2, 5). Minor-group HRVs are thus absolutely dependent on the low endosomal pH for infection to occur.

In previous work, investigators have begun to characterize the internalization pathway and mechanism of HRV2 uncoating in HeLa cells (35, 36, 41). Once internalized, native HRV2 is transferred to early endosomes, where it dissociates from its receptors at pHs of 6.5 to 6.0 (5). It further undergoes a structural modification of the capsid, giving rise to subviral particles with altered antigenicity. While native virus is D-antigenic, subviral particles are C-antigenic. These subviral particles comprise A particles which have lost VP4 and empty B particles which, in addition, have also lost the RNA (23, 24). Elevation of the endosomal pH by monensin (31) or by the vacuolar ATPase (V-ATPase) inhibitor bafilomycin A1 (35) prevents this process and completely inhibits infection. The structural transitions are thus required for RNA release and transport across the endosomal membrane into the cytosol (35, 36). In earlier work, Prchla et al. demonstrated that low-molecular-mass (10-kDa) dextran but not high-molecular-mass (70-kDa) dextran was released from isolated endosomes containing internalized virus upon exposure to low pH (36). These *in vitro* studies suggested that a pore of limited size was formed in the endosomal membrane and allowed the dextran to escape from the endosome. Conversion of the virus to the empty subviral B particle is accompanied by an iris-like movement of the five copies of VP1 at each of the 12 fivefold axes of icosahedral symmetry. This process creates a channel with an estimated diameter of 10 Å—large enough for RNA to escape (14). Concomitantly, the N terminus of VP1 and the entire VP4 are extruded and most likely interact with the endosomal membrane. As shown for poliovirus, B particles indeed attach to liposomes and, upon proteolytic digestion, a 3-kDa peptide remains with the liposome fraction and is protected against degradation (9). This molecular mass corresponds to the 30 N-terminal amino acids of VP1, the first 20 of which have a high propensity to form an amphipathic helix. Similar helices can also be constructed from the N termini of VP1 of several other picornaviruses (36), and a 24-amino-acid-long peptide from the N terminus of VP1 was shown to have liposome- and erythrocyte-disrupting activities (45).

Since these experiments were carried out either with virus in solution or with isolated endosomes, it was still unclear how RNA accesses the cytosol from endosomes during the *in vivo* infection pathway. In the present study, we addressed this question and observed HRV2 RNA release *in vivo* by using fluorescence-activated cell sorting (FACS) analysis and single-organelle flow analysis (SOFA). This study is based on a previously established assay that allows for monitoring of the release of a fluorescent (fluorescein isothiocyanate [FITC]-cyanine 5 [Cy5]) fluid-phase marker cointernalized with virus from endosomes into the cytosol (40). While the fluorescence of Cy5 is not affected by pH, FITC fluorescence is pH sensitive. When dextran is released from acidic endosomes into the pH-neutral cytosol, a change in pH occurs that can be monitored as the ratio of the fluorescence intensities of the respective markers (FITC to Cy5). The average pH of vesicles and the cytosol was analyzed by FACS analysis of intact cells, and the

pH of the labeled vesicles, together with their approximate number, was determined by SOFA of cell homogenates. We show here that an increase in the pH measured with high-molecular-mass dextran occurs upon adenovirus infection, whereas an increase in the pH upon HRV2 infection is observed only when low-molecular-mass dextran is cointernalized with the virus. These findings indicate that adenovirus ruptures the endosomal membrane, whereas HRV2 forms a pore, and strongly suggest that RNA enters the cytosol through a channel in the endosomal membrane as a consequence of exposure to low pH.

#### MATERIALS AND METHODS

**Chemicals.** All chemicals were obtained from Sigma (St. Louis, Mo.) unless specified otherwise. Bafilomycin A1 (Alexis, San Diego, Calif.) was dissolved in dimethyl sulfoxide at 20 mM and stored at  $-20^{\circ}\text{C}$ . In all experiments, the final concentration of dimethyl sulfoxide was kept below 1%. FITC-dextran with a molecular mass of 10 kDa or a molecular mass of 70 kDa was extensively dialyzed against Tris-buffered saline (pH 7.4) and finally against phosphate-buffered saline (pH 7.4) (PBS) before use. Cy5.18-OSu (Cy5) was obtained from Amersham Pharmacia Biotech, United Kingdom.

**Cell culture and viruses.** HeLa cells (Wisconsin strain; obtained from R. Rueckert, University of Wisconsin) were cultured in monolayers in minimum essential medium (MEM) supplemented with 10% heat-inactivated fetal calf serum and 2 mM L-glutamine. Cells in suspension were grown in Joklik's MEM containing 7% horse serum (all from GIBCO Invitrogen Corp., Paisley, United Kingdom) at  $37^{\circ}\text{C}$  with 5%  $\text{CO}_2$  in a humidified incubator. HRV2 was propagated as described previously (31). Adenovirus type 5 mutant *dl312* (Ad5), a replication-incompetent strain with a deletion in the E1a region, was propagated in 293 cells (11, 18).

**Preparation of Cy5-dextran conjugates.** A total of 10 mg of dextran (10 or 70 kDa) was dissolved in 2.4 ml of 0.1 M sodium bicarbonate buffer (pH 9.5). This solution was vigorously mixed with 100  $\mu\text{l}$  of Cy5 solution (1.0 mg of Cy5 dissolved in 140  $\mu\text{l}$  of dry dimethyl formamide) and incubated for 1 h at room temperature. Free Cy5 was removed by gel chromatography on a G-25 column. Labeled dextran was dialyzed against Tris-buffered saline and finally against PBS and stored at  $-20^{\circ}\text{C}$ .

**Labeling of HeLa cells with endocytic markers.** HeLa cells were grown in suspension to a density of  $2 \times 10^5/\text{ml}$  in MEM supplemented with 7% horse serum. Cells ( $2 \times 10^7$ ) then were preincubated in medium supplemented with 10% fetal calf serum for 30 min at  $37^{\circ}\text{C}$  or for 60 min at  $20^{\circ}\text{C}$ . Aliquots of the cells were used for determining the autofluorescence at pH 7.4 and for establishing the pH calibration curve (see below). Other aliquots were incubated with or without Ad5 (1,000 particles/cell) or HRV2 (1,000 50% tissue culture infective doses [TCID<sub>50</sub>]/cell), 6 mg of FITC-dextran/ml, and 0.6 mg of Cy5-dextran/ml for 20 or 60 min at the given temperatures. Internalization was halted by washing the cells with ice-cold PBS. Cells were pelleted; the cell pellet was resuspended in PBS and analyzed immediately by flow cytometry (for FACS analysis of intact cells, see Fig. 1). For SOFA, aliquots of the cells were homogenized with a ball-bearing homogenizer; the homogenate was centrifuged at  $270 \times g$  for 10 min to obtain the postnuclear supernatant (PNS), which was divided into aliquots to measure the endosomal pH and the number of fluorescent endosomes (40).

**Generation of a pH calibration curve by flow cytometry.** A pH calibration curve for internalized FITC- and Cy5-labeled dextran (FITC/Cy5-dextran) was generated by using aliquots of labeled cells as described previously (17). Buffers with pHs of between 5.0 and 7.5 were prepared by mixing 50 mM HEPES with 50 mM morpholineethanesulfonic acid; each buffer also contained 50 mM NaCl, 30 mM ammonium acetate, and 40 mM sodium azide. Cells were divided into eight aliquots, pelleted, resuspended in the various buffers, and equilibrated at  $4^{\circ}\text{C}$  for 10 min to deplete endogenous ATP and to inhibit V-ATPases. Equilibration of the intravesicular milieu with the external medium is accomplished with a weak acid-base buffer (39).

**Flow cytometry and determination of endosomal pH.** A dual-laser FACS-Calibur (Becton Dickinson Immunocytometry Systems) equipped with argon ion and red-diode lasers was used. FITC fluorescence (488-nm excitation) was determined by using a 530-nm band-pass filter (30-nm bandwidth), and Cy5 fluorescence (635-nm excitation) was determined by using a 661-nm band-pass filter (16-nm bandwidth). Forward scatter (FSC) and  $90^{\circ}$  side scatter (SSC), along with both fluorescence values, were collected in list mode at a 256-channel resolution.

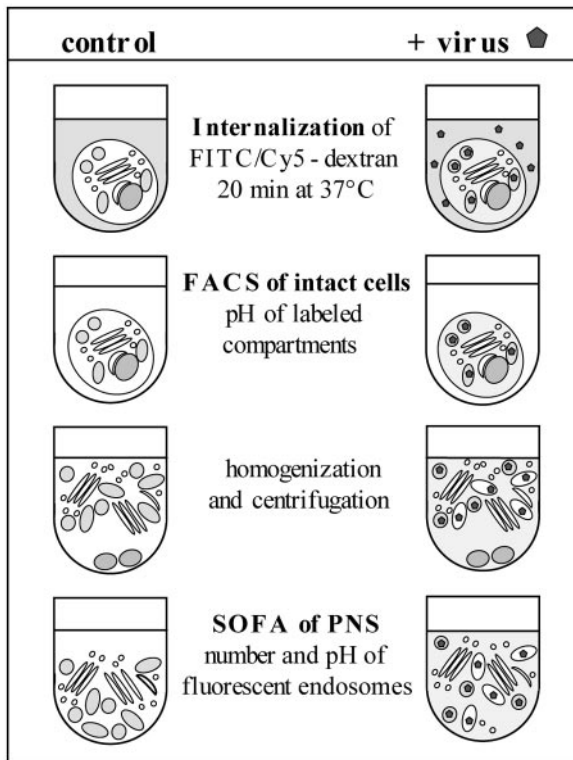


FIG. 1. Experimental setup for FACS analysis of intact cells and SOFA of cellular organelles. FITC/Cy5-dextran was internalized into HeLa cells in the absence of virus (left) and in the presence of virus for 20 min (right). Cells were cooled and washed, the fluorescence intensities of the two fluorophores were determined by FACS analysis of intact cells, and the FITC fluorescence/Cy5 fluorescence ratio was calculated. An aliquot of the control sample was used to obtain a calibration curve. The endosomal pH was equilibrated with buffers with known pHs in the presence of azide and ammonium acetate, and the fluorescence ratios of the fluorophores were plotted against the pHs. From this plot, the average pH of all labeled compartments in intact cells was derived. To selectively determine the pH (and the number) of the endocytic compartments, cells were homogenized and nuclei were removed by centrifugation to obtain a PNS. The PNS then was analyzed by SOFA.

For flow cytometry of cell suspensions, 10,000 cells were counted; 100,000 events per sample were collected for SOFA. Each sample was measured eight times; duplicate samples were used for pH calibration. The mean values for FITC fluorescence and Cy5 fluorescence were calculated for each sample, and the autofluorescence of unlabeled samples (see Fig. 2B) was subtracted. The ratios of FITC fluorescence to Cy5 fluorescence were converted into mean pHs by using the pH calibration curve (39).

**Definition of large endosomes.** The following parameters were defined. (i) The threshold for FSC and SSC was determined from an analysis of sheath fluid without a sample (see Fig. 2A, dark gray area); to differentiate large vesicles from small vesicles, an analysis window was set with the lower FSC value just above the maximum FSC value obtained for sheath fluid alone (see Fig. 2C) (40). (ii) Gates were determined by excluding all events recorded for the PNS of unlabeled HeLa cells in the dual-fluorescence mode (FITC fluorescence versus Cy5 fluorescence; see Fig. 2B). As a control, the total numbers of small and large endosomes in the PNS of cells whose endocytic vesicles had been labeled for 20 min with FITC/Cy5-dextran at 37°C were determined (see Fig. 2D). About 70% of the large vesicles (see Fig. 2E) but only 40% of the small vesicles (see Fig. 2F) were fluorescent. Thus, in the present work, only large vesicles were investigated, as selected by this gate. In total, 100,000 events (small and large vesicles) were measured, but only large vesicles were considered, and the number of fluorescent vesicles within this gate was set to 100% (in the absence of virus).

## RESULTS

**Experimental setup for the determination of pH and number of fluorescent endosomes by FACS analysis and SOFA.** A previously established two-step assay (40) allows for the determination of the influence of a virus on endosome integrity and pH. It is based on the internalization of the fluid-phase marker FITC/Cy5-dextran; this inert marker is nondegradable and labels all endocytic compartments (early endosomes, late endosomes, lysosomes and, to a lesser extent, recycling compartments) as a function of time and temperature. While Cy5 fluorescence is pH independent, FITC fluorescence decreases with pH (30, 39). The ratio of FITC fluorescence to Cy5 fluorescence is thus directly correlated with the pH.

The experimental setup is illustrated in Fig. 1. Labeled dextran is internalized in the absence or in the presence of the virus for 20 min. Free dextran is washed away with cold PBS, and the cell suspension is first analyzed by conventional FACS analysis. In the absence of virus, the ratio of FITC fluorescence to Cy5 fluorescence reflects the average pH of all endosomes labeled under this particular condition. Leakage of the marker from acidic endosomes into the pH-neutral cytosol, such as that caused by an endosome-disrupting virus, results in an increase in the FITC fluorescence/Cy5 fluorescence ratio. To selectively determine the number and pH of endosomes, an aliquot of the cells is homogenized, and the PNS is subjected to SOFA as illustrated in the lower panels in Fig. 1. The following parameters are determined at the same time: SSC versus FSC (SSC/FSC) which are related to size and optical density, and FITC fluorescence intensity versus Cy5 fluorescence intensity (FITC/Cy5) (29, 37).

Such an analysis of the PNS of unlabeled HeLa cells is depicted in Fig. 2A and B. All events arising from sheath fluid alone are shown in pink and were excluded. High values for FSC and SSC corresponded approximately to large vesicles (Fig. 2A; outside the sheath flow area). The FITC/Cy5 signal in Fig. 2B was entirely due to autofluorescence (background); therefore, gates (Fig. 2D to F) were always set to exclude these events. When the PNS from HeLa cells labeled with FITC/Cy5-dextran for 20 min was analyzed in the SSC/FSC mode (Fig. 2C), a size distribution similar to that of unlabeled cells was obtained (compare to Fig. 2A), whereas the diagram in Fig. 2D indicated the presence of FITC- and Cy5-labeled endosomes outside the area corresponding to autofluorescence. To differentiate between small and large vesicles, gates were set in the FSC mode just above the maximum value of the signal from sheath fluid alone. The distributions of fluorescent large and small endosomes labeled within 20 min when these gates were used are shown in Fig. 2E and F. From the total number of vesicles (100,000 events), about 70% of the large vesicles but only 40% of the small vesicles were fluorescent and thus, by definition, were endosomes.

Finally, the mean pH of a respective gated endosome population can be deduced from a pH calibration curve. An average pH of 5.8 was obtained for large endosomes. Based on size and low pH, this large-vesicle fraction consists preferentially of late endocytic compartments. It was demonstrated previously by cell fractionation and subcellular localization that within 20 min of internalization, HRV2 is found in late endosomes en route to lysosomes (3, 20, 35, 41). Uncoating and RNA release

**PNS of unlabeled HeLa cells      PNS of HeLa cells labeled with FITC/Cy5-dextran**

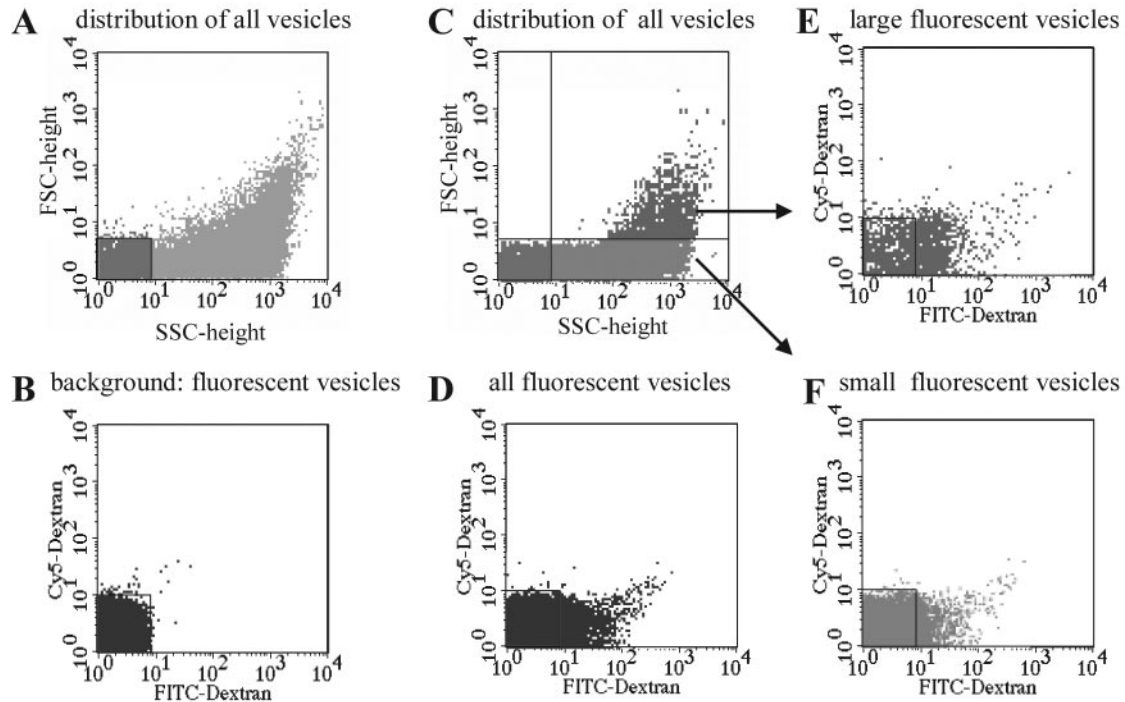


FIG. 2. SOFA and selection of gates. (A and B) The PNS from unlabeled HeLa cells was analyzed in SSC versus FSC mode (A) as well as in fluorescence mode (B). Regions corresponding to buffer and sheath fluid alone (A, dark gray area) and background fluorescence (B) were identified, and gates were set to exclude these events in the following experiments with labeled samples. (C to F) HeLa cells were labeled with 70-kDa FITC/Cy5-dextran for 20 min at 37°C, washed with ice-cold PBS, and homogenized, and the PNS was analyzed as described in Materials and Methods. (C) To differentiate large vesicles from small vesicles, an analysis window was created with the lower FSC value just above the maximum FSC value determined for sheath fluid alone. Large vesicles were defined as all events outside this window. (E and F) Distributions of large and small fluorescent vesicles (endosomes), respectively, determined with these gates. FITC- and Cy5-positive compartments were located outside the region corresponding to background fluorescence (squares at lower left). (D) Entire population of fluorescent vesicles (large plus small). The mean FITC fluorescence/Cy5 fluorescence ratio of the population of large endosomes was calculated, and the pH was determined by using a pH calibration curve. In the absence of virus, a mean pH of 5.8 was obtained.

occur in these late endocytic compartments (endosomal carrier vesicles and late endosomes). Therefore, this large-vesicle population was selected for analysis in all further experiments.

It was shown earlier by FACS analysis of HeLa cells that 30 min of incubation with a 200 nM concentration of the V-ATPase inhibitor bafilomycin A1 is required for the neutralization of dextran-labeled endosomes (3). Nevertheless, we verified in the two-step assay that this drug indeed raises the endosomal pH to neutrality under the specified conditions. Cells were preincubated without or with inhibitor and labeled for 20 min with FITC/Cy5-dextran. Determination of the endosomal pH by FACS analysis and SOFA revealed average pHs of 6.4 in intact cells and 5.8 in vesicles (Fig. 3). Note that the value obtained by FACS analysis of intact cells is the average pH of all labeled compartments, including (small) early (pHs 6.0 to 5.9), (large) late (pHs 5.5 to 5.0), and recycling (pHs above 6.4) compartments. However, in the SOFA experiments, we set the gate for large compartments; hence, predominantly late compartments with lower pHs were analyzed. Consequently, the mean pH determined by FACS analysis is approximately 0.8 U higher than that obtained by SOFA.

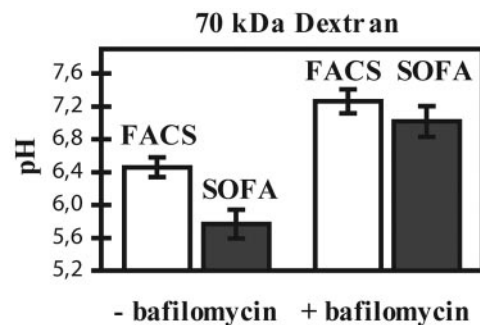


FIG. 3. Effect of bafilomycin A1 on endosomal pH as determined by FACS analysis and SOFA. HeLa cells were preincubated in the absence or in the presence of 200 nM bafilomycin A1 for 30 min at 37°C, transferred to fresh medium containing FITC/Cy5-dextran (70 kDa) without or with bafilomycin A1, and further incubated for 20 min. Cells were cooled and washed with PBS, and an aliquot was subjected to FACS analysis. The remaining cells were homogenized, and a PNS was prepared and analyzed by SOFA. The pH was calculated by using a pH calibration curve (see Materials and Methods). For SOFA, only large vesicles were considered. The mean and standard error of the mean for 13 experiments with eight measurements each are shown.

The pH increased above 7.0 upon preincubation with bafilomycin A1 regardless of the method of analysis (Fig. 3).

**Ad5 ruptures endocytic vesicles in a pH-independent manner.** It is well established that adenovirus ruptures the endosomal membrane (27) and, as shown previously, the number of vesicles ruptured can be quantified by using a two-step assay involving FACS analysis and SOFA (40). Therefore, Ad5 was included in all experiments as a control for the virus-induced release of the fluid-phase marker from endosomes. Further, we wanted to assess the effect of bafilomycin A1 on Ad5-mediated endosomal rupture, since contradictory results on the effect of pH on this process have been reported (8, 12, 34, 38, 44). Ad5 was cointernalized with labeled dextran for 20 min at 37°C, and the pH of labeled compartments in intact cells was determined by FACS analysis. Mock-infected cells (control) had an average pH of 6.4, while cells that had internalized Ad5 had a pH of about 7.1, a value significantly higher than the control value (Fig. 4A). These data agree well with the contention that endosomes released dextran into the cytoplasm in the presence of adenovirus. The number of large vesicles containing FITC/Cy5-dextran was determined by SOFA and was set to 100% in the absence of virus. As depicted in Fig. 4B, Ad5 decreased the number of fluorescent endosomes by nearly 40%. Thus, about 60% of the vesicle population remained intact. Next, the pH of the residual endosome population was calculated from the SOFA data above. The values were virtually identical in the presence and in the absence of the virus, suggesting that the virus by itself does not change the pH of endosomes that still contain the marker (Fig. 4C). When Ad5 was internalized in the absence or in the presence of bafilomycin A1 and the number of fluorescent endosomes was determined by SOFA as described above, no difference was seen (Fig. 4B). Thus, raising the endosomal pH to neutrality (Fig. 3) did not affect adenovirus-induced endosomal rupture.

**HRV2 uncoating does not affect endosome integrity.** The method described above, as validated with Ad5, allows for the determination of (i) the pH of labeled compartments in intact cells (FACS analysis), (ii) the endosomal pH (SOFA), and (iii) the endosome integrity on the basis of the number of fluorescent endosomes (SOFA). We studied these parameters for HRV2 entry by using dextran with a low or a high molecular mass as a fluid-phase marker to allow for the detection of pores eventually opening during virus uncoating. HRV2 was cointernalized with FITC/Cy5-labeled dextran for 5 and 20 min at 34°C, the optimal growth temperature of rhinoviruses. At these times, the virus localizes to early and late endosomes, respectively (20, 41). The following experiments were conducted in parallel with internalization of either 10- or 70-kDa FITC/Cy5-dextran in the absence or in the presence of HRV2. With 70-kDa dextran, virtually no difference in the pHs of labeled compartments in intact cells between mock-infected and HRV2-infected cells was observed by FACS analysis with internalization for 20 min (Fig. 5A). Obviously, the vesicles remain intact, although the viral RNA arrives in the cytoplasm, since productive uncoating occurs within this time frame (17). With 10-kDa dextran, the pHs of labeled compartments in intact cells increased by one pH unit over the pH in the control incubation (i.e., without virus). Conversely, when the pH in intact cells was measured 5 min after internalization, it was found to be unaffected by the presence of the virus (Fig. 5B).

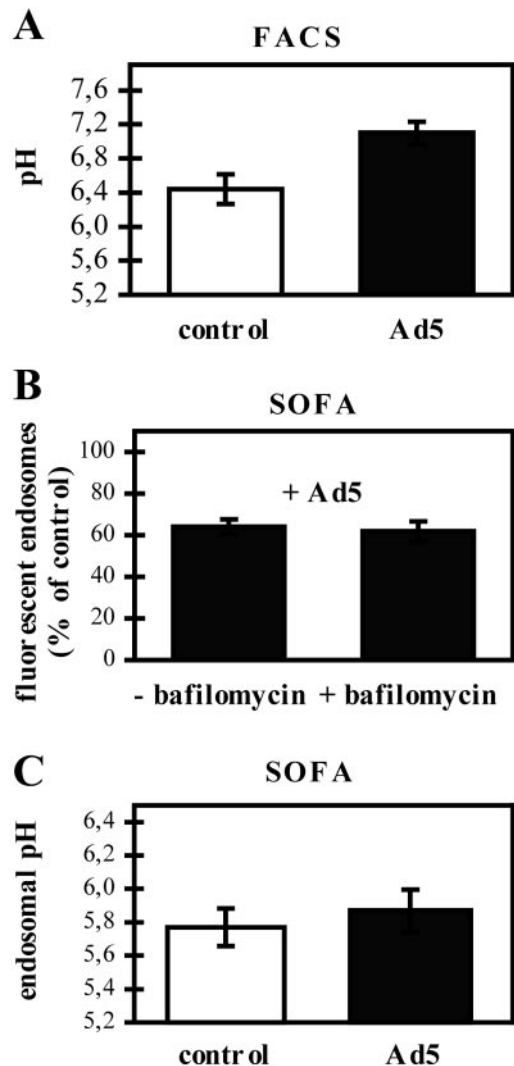


FIG. 4. Ad5 ruptures endosomes regardless of the presence of bafilomycin A1. (A) FITC/Cy5-dextran (70 kDa) was internalized into HeLa cells in the absence of Ad5 (control) or in the presence of Ad5 (1,000 viral particles per cell) for 20 min at 37°C. The mean pH of labeled compartments in intact cells was calculated from the fluorescence ratio determined by FACS analysis by using a pH calibration curve. Data are the mean and standard error of the mean for 22 experiments with eight parallel determinations. (B) HeLa cells were preincubated without or with 200 nM bafilomycin A1 for 30 min at 37°C. FITC/Cy5-dextran was internalized in the absence of Ad5 (control) or in the presence of Ad5 for 20 min at 37°C without or with bafilomycin A1. Cells were homogenized, and a PNS was analyzed by SOFA. The number of large fluorescent endosomes is shown and is expressed as a percentage of the value for the respective control. Data are the mean and standard error of the mean for 16 individual experiments with eight parallel determinations. (C) The pH of fluorescent endosomes shown in panel B in the absence or in the presence of virus was calculated by using the pH calibration curve. Data are the mean and standard error of the mean for four experiments with eight parallel determinations.

This finding indicates that 10-kDa dextran was released into the pH-neutral cytoplasm from late but not from early endosomes in the presence of HRV2 but that 70-kDa dextran was retained. Note that the pHs determined in the absence of virus

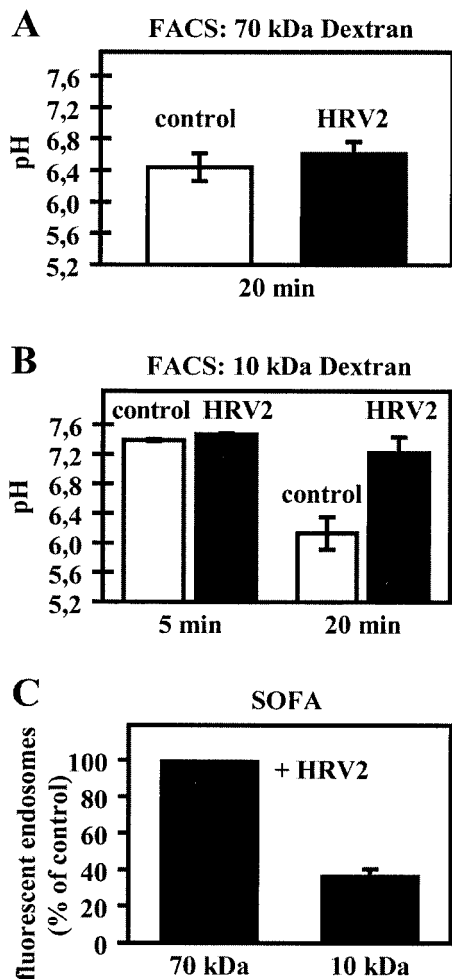


FIG. 5. HRV2 differentially affects the pHs of compartments labeled with 70- and 10-kDa dextrans. Internalization of the respective dextran was carried out in the absence of HRV2 (control) or in the presence of HRV2 at 1,000 TCID<sub>50</sub>/cell at 34°C. (A) Data obtained with 70-kDa FITC/Cy5-dextran internalized for 20 min. (B) Data obtained with 10-kDa FITC/Cy5-dextran internalized for 5 and 20 min. The pH of labeled compartments in intact cells was calculated from the data obtained by FACS analysis (A and B). Data are the mean and standard error of the mean for three individual experiments with eight parallel determinations. (C) Cells from panels A and B (right panels) were homogenized, and the PNS was analyzed by SOFA. Data are expressed as a percentage of the value for the respective control and are the mean and standard error of the mean for three individual experiments, with each sample being measured eight times.

for 20 min with 10- and 70-kDa dextrans were indistinguishable (Fig. 5A and B). This finding demonstrates that both dextrans localized to endosome populations with similar pHs.

Next, aliquots of the cells were homogenized, and the respective PNS was analyzed by SOFA. In the FSC/SSC mode, the total numbers of vesicles were similar for all conditions (70-kDa dextran without or with virus or 10-kDa dextran without or with virus; data not shown), indicating that the number of endosomes was unaffected by the virus. In the FITC/Cy5 mode, the number of fluorescent vesicles is determined. In the presence of HRV2, this analysis revealed a substantial difference between the 10-kDa dextran sample and the 70-kDa dex-

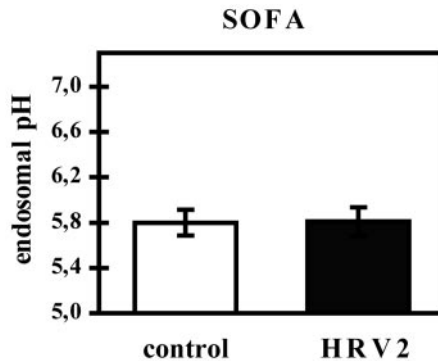


FIG. 6. The pH of intact endosomes is unchanged by HRV2. Seventy-kilodalton FITC/Cy5-dextran was internalized into HeLa cells for 20 min in the absence of HRV2 (control) or in the presence of HRV2 at 34°C. Cells were homogenized, a PNS was prepared, and the endosomal pH was determined by SOFA. Each experiment was carried out four times, with each sample being measured eight times; data are the mean and standard error of the mean.

tran sample (Fig. 5C). The number of endosomes labeled with 10-kDa FITC/Cy5-dextran was decreased by 64% compared to the value for the control sample (absence of virus), whereas the number of endosomes labeled with 70-kDa FITC/Cy5-dextran was unaffected by the virus (Fig. 5C). Since the total number of vesicles determined in the SSC/FSC mode was unaffected by HRV2, these results indicate that the endosomes remained impermeable to 70-kDa dextran, whereas low-molecular-mass dextran escaped into the cytoplasm as a consequence of HRV2 uncoating. These findings strongly suggest that pores of limited size just allowing for the escape of a low- but not of a high-molecular-mass marker are formed in the endosomal membrane upon HRV2 uncoating.

**HRV2 uncoating does not affect endosomal pH.** Since the “leakiness” of the endosomal membrane might also lead to dissipation of the endosomal pH gradient, we next calculated the pH of the endosome population labeled with 70-kDa FITC/Cy5-dextran from the SOFA experiment described above. With a calibration curve, a pH of about 5.8 was found in endosomes in the absence as well as in the presence of HRV2 (Fig. 6). This pH represents the average pH of all vesicles containing the dextran, i.e., predominantly late endosomes. It is surprising that no change in pH was observed even though 10-kDa dextran was lost from 64% of the endosomes under otherwise identical conditions, as shown in Fig. 5C.

**HRV2 RNA is released at 20°C.** Membrane fluidity is substantially reduced at lower temperatures, as reflected by the inhibition of many vesicular transport processes. Therefore, experiments aimed at characterizing events taking place in endosomes but not in lysosomes are often carried out at 20°C in order to prevent the delivery of endosomal cargo to lysosomes (13). A structural change from native virus to subviral A and B particles occurs at 20°C in vitro as well as when the virus is internalized for 2 h at 20°C (35); these data indicate that RNA is released but do not demonstrate its transport to the cytosol. We thus wondered whether the size-specific release of FITC/Cy5-dextran would also take place at this temperature; such release would be indicative of RNA gaining access to the cytoplasm. Cells were allowed to cointernalize HRV2 and 10-

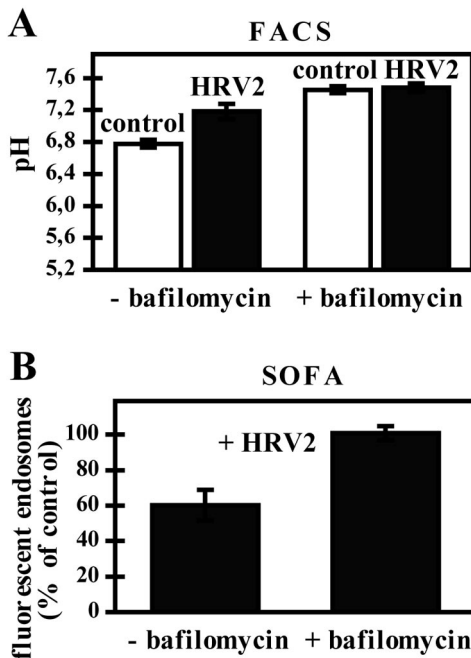


FIG. 7. RNA release from HRV2 occurs at 20°C. (A) HeLa cells were preincubated in the absence or in the presence of 200 nM bafilomycin A1 for 30 min at 20°C. Next, 10-kDa FITC/Cy5-dextran was internalized for 120 min at 20°C (without or with the drug and without or with HRV2). Cells were washed, and the pH of labeled compartments in intact cells was determined by FACS analysis. (B) Subsequently, the cells were homogenized, and the number of fluorescent endosomes in the PNS was determined by SOFA. Data are the mean and standard error of the mean for three individual experiments, with each sample being measured eight times.

kDa FITC/Cy5-dextran for 120 min at 20°C. The longer incubation time was chosen to compensate for the slower endocytosis rate at this temperature. Next, the pH of the cell suspensions was determined. As in the experiment carried out at 34°C (Fig. 5B), the pH in control cells (internalization in the absence of HRV2) was significantly lower than that in cells having internalized the virus (Fig. 7A). The number of fluorescent endosomes, as determined by SOFA, was reduced by 40%, demonstrating a size-dependent release of dextran. Therefore, it is highly likely that RNA also can leave endosomes at 20°C and gain access to the cytoplasm.

Bafilomycin A1 completely blocks the conformational change and HRV2 uncoating and infection irrespective of the internalization temperature (31, 35). When the same experiment was carried out in the presence of bafilomycin A1, the endosomal pH was raised to neutrality (Fig. 7A), and the number of fluorescent endosomes was unaffected by the virus when the drug was present (Fig. 7B). Bafilomycin A1 itself had no influence on the total number of endosomes (data not shown). These data clearly demonstrate that HRV2 also permeabilizes endosomes at 20°C, allowing for the exit of low-molecular-mass dextran, a process that is completely inhibited by bafilomycin A1. From these data it can be concluded that RNA penetration into the cytoplasm takes place even at 20°C.

## DISCUSSION

Prchla et al. developed an *in vitro* assay to determine the leakage of biotinylated dextran from isolated endosomes induced by the cointernalization of a given virus and low pH (36). With this method, low-molecular-mass (10-kDa) dextran and high-molecular-mass (70-kDa) dextran were shown to be released into the medium in a low-pH-dependent manner when adenovirus was cointernalized. These data were in good agreement with the well-documented endosomal rupture by this virus (27). In the present work, we investigated the *in vivo* situation and analyzed dextran release as a consequence of the early steps in viral infection by measuring the pHs of the compartments containing the cointernalized fluid-phase marker. FITC/Cy5-dextran was cointernalized into HeLa cells, and the pH was derived from the ratio of the fluorescence intensities of the pH-sensitive FITC and the pH-insensitive Cy5 as measured in intact cells by FACS analysis and in endosomes in a PNS by SOFA (Fig. 1). In agreement with the earlier *in vitro* results, we found that dextran gained access to the pH-neutral cytosol when adenovirus was cointernalized. However, dextran release by adenovirus was not pH dependent, since it occurred irrespective of the presence of the V-ATPase inhibitor bafilomycin A1 (Fig. 4).

Data on the pH dependence of adenovirus penetration and infection are conflicting; lysosomotropic agents such as  $\text{NH}_4\text{Cl}$  were shown to inhibit (12) or not to inhibit (38) infection by Ad2. Further, Ad5 was demonstrated to require pH 6.0 for endosome lysis (28), whereas Perez and Carrasco (34) showed that infection with adenovirus occurred in the presence of 1  $\mu\text{M}$  bafilomycin A1. In addition, numerous *in vitro* experiments demonstrated low-pH-dependent adenovirus plasma membrane permeabilization (e.g., references 42 and 44), whereas unpublished data from U. Greber et al. showed that Ad2 entry is not affected by bafilomycin A1 but is inhibited by  $\text{NH}_4\text{Cl}$  or monensin. We believe that this discrepancy is largely due to the virus using two parallel internalization pathways involving macropinosomes and endosomes (26). Depending on the cell type, the metabolic state of the cells, and experimental conditions, one or the other pathway might be dominant.

In the experiments described in this article, we concentrated on large vesicles. These not only include endosomes but also might include macropinosomes. We believe that our present experiments more closely reflect the physiologic situation than previous experiments with isolated endosomes that were presumably depleted of macropinosomes. In the latter situation, only pH-dependent release *in vitro* was monitored, but pH-independent release might have already occurred to a substantial extent during the internalization process (36).

The same experiments carried out with HRV2 showed the release of 10-kDa dextran only and required acidification of the endosomal lumen. In contrast to the data for adenovirus, the results obtained with HRV2 *in vitro* (36) and *in vivo* (Fig. 5 and 6) were both in agreement with the formation of size-selective pores upon exposure of the virus to low pHs. Thus, the formation of these pores is strictly low-pH dependent, as deduced from its inhibition by bafilomycin A1 (Fig. 7). Seventy-kilodalton dextran was not released under otherwise identical conditions. This result might be explained by the blockage of membrane permeabilization by 70-kDa dextran. However,

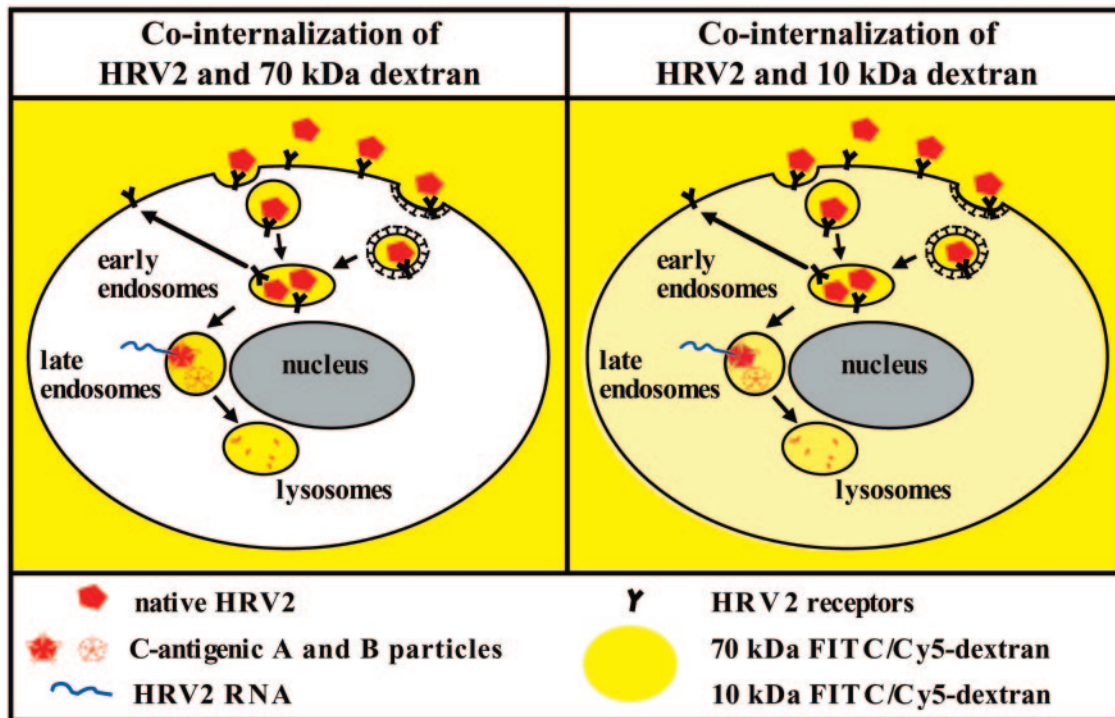


FIG. 8. Schematic representation of endosomal penetration of HRV2 and release of markers with different molecular masses. Following HRV2 binding to its receptors and cointernalization of the fluid-phase marker, the cargo is delivered to early endosomes, where virus-receptor dissociation takes place. Receptors are recycled, whereas HRV2 is transported to late endosomes, where it undergoes conformational modifications at pHs below 5.6, accompanied by RNA release. Cointernalized dextran is released from the endosomes into the cytosol only if it is small enough (10 kDa) to pass through pores opened in the endosomal membrane by viral proteins. RNA-free B particles are finally delivered to and degraded in lysosomes.

this possibility can be excluded on the basis of experiments in which virus was cointernalized with dextran and 80S particles were found in isolated endosomes (35).

The present data demonstrate that for HRV2, the uncoating process indeed involves the generation of pores in endosomes (Fig. 8). It is remarkable that 10-kDa dextran was released but that no change in the endosomal pH was noted (Fig. 6). These results might be explained in two ways. First, V-ATPases are sufficiently active so as to compensate for eventual proton leaks or other changes in cation or anion permeabilities. This scenario is in agreement with the results of *in vitro* acidification assays, in which the addition of the proton ionophore carbonyl cyanide *p*-trifluoromethoxyphenylhydrazone only slightly affected ATP-dependent acidification and steady-state pH (10). The second explanation, which appears to be more likely, is that pores generated during the release of viral RNA (and 10-kDa dextran) close thereafter, so that the proton gradient can be reestablished. We have not explicitly shown the penetration of viral RNA into the cytosol. However, under the conditions used in these assays at 20°C as well as at 34°C, subviral 80S particles were generated and were found in isolated endosomes (20, 35). These particles are the end products of the uncoating reaction, they constitute empty capsids without VP4 and RNA, and they are seen to occur *in vivo* after 10 min (22, 23). Hence, virus localization in late endosomes, the production of 80S particles, and pore formation occur within the same time frame.

The overall integrity of the endosomal membrane is main-

tained, but the escape of 10-kDa dextran indicates at least transient leakiness. What is the nature of the pores? In principle, two possibilities can be envisioned. The first possibility is the generation of pores contiguous with the viral capsid. Subviral 135S particles are hydrophobic due to the exposure of the amphiphilic N termini of VP1 (21). Therefore, a channel connecting the viral interior with the pores in the endosomal membrane might be formed. Alternatively, the released VP4 molecules might be inserted into the membrane and by themselves generate a channel. We cannot differentiate between the flow of dextran through the remnant of the virus particle and direct passage through the membrane. The holes at the fivefold axes of 80S particles are about 10 Å in diameter. This diameter is sufficient for the passage of RNA in an unfolded state, which has approximately the same diameter. However, the hydrodynamic diameters of dextran molecules are 16 Å for 10-kDa dextran and 40 Å for 70-kDa dextran (7), and the passage of even small dextran would be slow. Therefore, we must consider the possibility either that the particle can make larger holes due to breathing or that the particle falls off the membrane and thereby makes the pores in the membrane more accessible.

For poliovirus, the importance of the N terminus of VP1 as well as VP4 for the uncoating process has been clearly demonstrated (19), and the formation of pores in artificial lipid bilayers has been shown (6). Also, low-pH-dependent cytoplasmic delivery of the toxin sarcin is promoted under conditions where poliovirus uncoating can take place (1). However, poliovirus infects in a low-pH-independent manner, and the site

of uncoating is still unclear. Therefore, no direct correlation between sarcin entry and the site and mode of poliovirus uncoating is obvious.

In contrast to data for poliovirus, for which it was not possible to distinguish between membrane destabilization or membrane lysis and pore formation (6), our study demonstrates the low-pH-dependent formation of size-selective pores for the penetration of HRV2 RNA from the endosome into the cytosol, as detailed in Fig. 8. Upon binding to its receptors, HRV2 is cointernalized with the fluid-phase marker and is delivered to early endosomes. The mildly low pH in these compartments results in the dissociation of virus-receptor complexes, allowing for receptor recycling and virus transport to late endosomes. In the pH environment of late endosomes (pHs of <5.6), the virus undergoes conformational modifications resulting in the generation of subviral 80S particles and RNA release. Ten-kilodalton dextran passes into the cytosol through pores opened in the endosomal membrane through interactions with hydrophobic regions in viral proteins. These pores are presumably used by RNA for entry into the cytosol but are too small for 70-kDa dextran to pass through. These data are in excellent agreement with the results of previous studies using isolated endosomes and assessing subviral particle formation (35, 36).

#### ACKNOWLEDGMENTS

This work was supported by Austrian Science Fund grants P 10617-GEN and P 17590 to R.F.

#### REFERENCES

- Almela, M., M. Gonzalez, and L. Carrasco. 1991. Inhibitors of poliovirus uncoating efficiently block the early membrane permeabilization induced by virus particles. *J. Virol.* **65**:2572–2577.
- Baravalle, G., L. Snyers, M. Brabec, D. Blaas, and R. Fuchs. 2004. Human rhinovirus type 2-antibody complexes enter and infect cells via Fc-gamma receptor IIB1. *J. Virol.* **78**:2729–2735.
- Bayer, N., D. Schober, E. Prchla, R. F. Murphy, D. Blaas, and R. Fuchs. 1998. Effect of bafilomycin A1 and nocodazole on endocytic transport in HeLa cells: implications for viral uncoating and infection. *J. Virol.* **72**:9645–9655.
- Blaas, D., and R. Fuchs. 1999. Early steps in rhinoviral infection. *Recent Res. Dev. Virol.* **1**:485–503.
- Brabec, M., G. Baravalle, D. Blaas, and R. Fuchs. 2003. Conformational changes, plasma membrane penetration, and infection by human rhinovirus type 2: role of receptors and low pH. *J. Virol.* **77**:5370–5377.
- Danthi, P., M. Tosteson, Q. H. Li, and M. Chow. 2003. Genome delivery and ion channel properties are altered in VP4 mutants of poliovirus. *J. Virol.* **77**:5266–5274.
- Ekani-Nkodo, A., and D. K. Fygenson. 2003. Size exclusion and diffusion of fluoresceinated probes within collagen fibrils. *Phys. Rev. E Stat. Nonlin. Soft Matter Phys.* **67**:021909.
- Everitt, E., and E. Rodriguez. 1999. Adenovirus cellular receptor site recirculation of HeLa cells upon receptor-mediated endocytosis is not low pH-dependent. *Arch. Virol.* **144**:787–795.
- Fricks, C., and J. Hogle. 1990. Cell-induced conformational change in poliovirus: externalization of the amino terminus of VP1 is responsible for liposome binding. *J. Virol.* **64**:1934–1945.
- Fuchs, R., P. Male, and I. Mellman. 1989. Acidification and ion permeabilities of highly purified rat liver endosomes. *J. Biol. Chem.* **264**:2212–2220.
- Graham, F., J. Smiley, W. Russell, and R. Nairn. 1977. Characteristics of a human cell line transformed by DNA from human adenovirus type 5. *J. Gen. Virol.* **36**:59–74.
- Greber, U., M. Willetts, P. Webster, and A. Helenius. 1993. Stepwise dismantling of adenovirus 2 during entry into cells. *Cell* **75**:477–486.
- Griffiths, G., B. Hoflack, K. Simons, I. Mellman, and S. Kornfeld. 1988. The mannose 6-phosphate receptor and the biogenesis of lysosomes. *Cell* **52**:329–341.
- Hewat, E., E. Neumann, and D. Blaas. 2002. The concerted conformational changes during human rhinovirus 2 uncoating. *Mol. Cell* **10**:317–326.
- Hofer, F., M. Gruenberger, H. Kowalski, H. Machat, M. Huettinger, E. Kuechler, and D. Blaas. 1994. Members of the low density lipoprotein receptor family mediate cell entry of a minor-group common cold virus. *Proc. Natl. Acad. Sci. USA* **91**:1839–1842.
- Hogle, J. M. 2002. Poliovirus cell entry: common structural themes in viral cell entry pathways. *Annu. Rev. Microbiol.* **56**:677–702.
- Huber, M., M. Brabec, N. Bayer, D. Blaas, and R. Fuchs. 2001. Elevated endosomal pH in HeLa cells overexpressing mutant dynamin can affect infection by pH-sensitive viruses. *Traffic* **2**:727–736.
- Jones, N., and T. Shenk. 1979. An adenovirus type 5 early gene function regulates expression of other early viral genes. *Proc. Natl. Acad. Sci. USA* **76**:3665–3669.
- Kirkegaard, K. 1990. Mutations in VP1 of poliovirus specifically affect both encapsidation and release of viral RNA. *J. Virol.* **64**:195–206.
- Kronenberger, P., D. Schober, E. Prchla, D. Blaas, and R. Fuchs. 1997. Use of free-flow electrophoresis for the analysis of cellular uptake of picornaviruses. *Electrophoresis* **18**:2531–2536.
- Lonberg-Holm, K., L. B. Gosser, and J. Shimshick. 1976. Interaction of liposomes with subviral particles of poliovirus type 2 and rhinovirus type 2. *J. Virol.* **19**:746–749.
- Lonberg-Holm, K., and B. D. Korant. 1972. Early interaction of rhinoviruses with host cells. *J. Virol.* **9**:29–40.
- Lonberg-Holm, K., and J. Noble-Harvey. 1973. Comparison of in vitro and cell-mediated alteration of a human rhinovirus and its inhibition by sodium dodecyl sulfate. *J. Virol.* **12**:819–824.
- Lonberg-Holm, K., and N. M. Whiteley. 1976. Physical and metabolic requirements for early interaction of poliovirus and human rhinovirus with HeLa cells. *J. Virol.* **19**:857–870.
- Marsh, M., and A. Pelchen-Matthews. 1993. Entry of animal viruses into cells. *Rev. Med. Virol.* **3**:173–185.
- Meier, O., K. Boucke, S. V. Hammer, S. Keller, R. P. Stidwill, S. Hemmi, and U. F. Greber. 2002. Adenovirus triggers macropinocytosis and endosomal leakage together with its clathrin-mediated uptake. *J. Cell Biol.* **158**:1119–1131.
- Meier, O., and U. F. Greber. 2003. Adenovirus endocytosis. *J. Gene Med.* **5**:451–562.
- Miyazawa, N., R. G. Crystal, and P. L. Leopold. 2001. Adenovirus serotype 7 retention in a late endosomal compartment prior to cytosol escape is modulated by fiber protein. *J. Virol.* **75**:1387–1400.
- Murphy, R. F. 1985. Analysis and isolation of endocytic vesicles by flow cytometry and sorting: demonstration of three kinetically distinct compartments involved in fluid-phase endocytosis. *Proc. Natl. Acad. Sci. USA* **82**:8523–8526.
- Murphy, R. F., S. Powers, and C. R. Cantor. 1984. Endosome pH measured in single cells by dual fluorescence flow cytometry: rapid acidification of insulin to pH 6. *J. Cell Biol.* **98**:1757–1762.
- Neubauer, C., L. Frasel, E. Kuechler, and D. Blaas. 1987. Mechanism of entry of human rhinovirus 2 into HeLa cells. *Virology* **158**:255–258.
- Nurani, G., B. Lindqvist, and J. M. Casasnovas. 2003. Receptor priming of major group human rhinoviruses for uncoating and entry at mild low-pH environments. *J. Virol.* **77**:11985–11991.
- Perez, L., and L. Carrasco. 1993. Entry of poliovirus into cells does not require a low-pH step. *J. Virol.* **67**:4543–4548.
- Perez, L., and L. Carrasco. 1994. Involvement of the vacuolar H(+)-ATPase in animal virus entry. *J. Gen. Virol.* **75**:2595–2606.
- Prchla, E., E. Kuechler, D. Blaas, and R. Fuchs. 1994. Uncoating of human rhinovirus serotype 2 from late endosomes. *J. Virol.* **68**:3713–3723.
- Prchla, E., C. Plank, E. Wagner, D. Blaas, and R. Fuchs. 1995. Virus-mediated release of endosomal content in vitro: different behavior of adenovirus and rhinovirus serotype 2. *J. Cell Biol.* **131**:111–123.
- Radcliff, G., and M. J. Jaroszeski. 1998. Basics of flow cytometry. *Methods Mol. Biol.* **91**:1–24.
- Rodriguez, E., and E. Everitt. 1996. Adenovirus uncoating and nuclear establishment are not affected by weak base amines. *J. Virol.* **70**:3470–3477.
- Rybak, S., and R. Murphy. 1998. Primary cell cultures from murine kidney and heart differ in endosomal pH. *J. Cell. Physiol.* **176**:216–222.
- Schober, D., N. Bayer, R. F. Murphy, E. Wagner, and R. Fuchs. 1999. Establishment of an assay to determine adenovirus-induced endosome rupture required for receptor-mediated gene delivery. *Gene Ther. Mol. Biol.* **3**:25–33.
- Schober, D., P. Kronenberger, E. Prchla, D. Blaas, and R. Fuchs. 1998. Major and minor receptor group human rhinoviruses penetrate from endosomes by different mechanisms. *J. Virol.* **72**:1354–1364.
- Seth, P., M. Willingham, and I. Pastan. 1985. Binding of adenovirus and its external proteins to Triton X-114. Dependence on pH. *J. Biol. Chem.* **260**:14431–14434.
- Uncapher, C. R., C. M. Dewitt, and R. J. Colonna. 1991. The major and minor group receptor families contain all but one human rhinovirus serotype. *Virology* **180**:814–817.
- Wickham, T. J., E. J. Filardo, D. A. Chereshe, and G. R. Nemerow. 1994. Integrin alpha v beta 5 selectively promotes adenovirus mediated cell membrane permeabilization. *J. Cell Biol.* **127**:257–264.
- Zauner, W., D. Blaas, E. Kuechler, and E. Wagner. 1995. Rhinovirus-mediated endosomal release of transfection complexes. *J. Virol.* **69**:1085–1092.